Journal of Magnetism and Magnetic Materials 395 (2015) 263–270

Contents lists available at ScienceDirect

Journal of Magnetism and Magnetic Materials

journal homepage: www.elsevier.com/locate/jmmm

Investigation of structural and magnetic properties of nanocrystalline Mn-doped $SrFe_{12}O_{19}$ prepared by proteic sol–gel process

W.M.S. Silva [a], N.S. Ferreira [b], J.M. Soares [c], R.B. da Silva [c], M.A. Macêdo [a,*]

[a] Physics Department, Federal University of Sergipe, São Cristóvão 49100-000, Brazil
[b] Departamento de Física, Universidade Federal do Amapá, Macapá 68902-280, Brazil
[c] Departamento de Física, Universidade do Estado do Rio Grande do Norte, Mossoró, RN 59610-210, Brazil

ARTICLE INFO

Article history:
Received 22 May 2015
Received in revised form
21 July 2015
Accepted 25 July 2015
Available online 28 July 2015

Keywords:
M-type hexaferrite
Proteic sol–gel process
Crystal structure
Magnetic property

ABSTRACT

Nanoparticles of $SrFe_{12-x}Mn_xO_{19}$ ($x=0.0$ and 0.10) were synthesized by a proteic sol–gel process. Thermogravimetric and differential thermal analyses (TG–DTA) indicated the formation of nanocrystalline strontium ferrite phase at a calcination temperature of 1000 °C. Structural and microstructural evolutions of the samples were studied by X-ray powder diffraction (XRD) and the Rietveld method. XRD patterns demonstrated that all samples consisted of single-phase M-type strontium *hexaferrite*. The crystal lattice constant did not change significantly with manganese substitution, ranging from 0.5877(3) nm ($x=0.0$) to 0.5876(3) nm ($x=1.0$). In addition, the average crystallite size, which was determined from the Williamson–Hall formula, was about 46.4–52.6 nm. Infrared spectroscopy (FT-IR) showed the presence of three principal absorption bands in the frequency ranges around 435–535 cm^{-1} and around 595 cm^{-1}, indicating the formation of the hexaferrite. Scanning electron microscopy (SEM) revealed that particles consisted of irregular platelets with sizes from 68 to 204 nm. Room-temperature Mössbauer investigations revealed that manganese ions preferentially occupied the 12k, $4f_1$, $4f_2$, and 2a sites. Hysteresis loops (M–H) showed that the saturation magnetization, remanence, and coercivity decreased with manganese doping. This effect is discussed in terms of the distribution of metal cations in the tetrahedral and octahedral sites.

1. Introduction

In recent years, M-type strontium hexaferrite (Sr-hexaferrite, $SrFe_{12}O_{19}$, SrM) has been the subject of extensive research due to its possible use in different technological applications. These materials are used in the magnetic recording industry and in magneto-optic devices, microwave devices, microelectromechanical systems, transformer cores, and antennas [1].

The physical properties of strontium ferrite depend intrinsically on the synthesis route. Strontium hexaferrite is a ferromagnetic material having a structure belonging to the hexagonal space group $P6_3/mmc$ and a magnetocrystalline anisotropy parallel to the c-axis of the unit cell. The crystalline structure of Sr-hexaferrite is constructed from a periodic repetition of SRS*R*blocks, where the cubic S block has a spinel structure and the hexagonal R block contains a Sr^{2+} ion, and the S* and R* blocks are axially symmetric around the hexagonal axis-*c* by 180°. Twenty-four Fe^{3+} ions occupy interstitial positions in five different crystallographic sites and are distributed as follows. Three octahedral sites (12k, $4f_2$, and 2a) and site $4f_1$ have a geometric tetrahedron formed by oxygen atoms. Site 2b has a bipyramidal geometry with a hexahedral triangular base formed by five oxygen atoms around the Fe^{3+} ion [2]. Numerous researchers [3,4] have been working on the effect of substitution of Fe^{3+} ions with different compounds, where the partial replacement of these ions modifies various magnetic properties [5,6].

Herein, we present a study of the effect of substitution of Fe^{3+} by Mn^{3+} on the structural and magnetic properties of strontium hexaferrite synthesized by the proteic sol–gel process.

2. Experimental

2.1. Synthesis

M-type $SrFe_{12-x}Mn_xO_{19}$ ($x=0$ and 0.10) samples were synthesized by the proteic sol–gel process. Appropriate amounts of Fe $(NO_3)_3 \cdot 9H_2O$ (99% Sigma-Aldrich), $Sr(NO_3)_3$ (99% Sigma-Aldrich),

* Corresponding author.
E-mail addresses: waldsonmarceloss@yahoo.com.br (W.M.S. Silva), odecamm@gmail.com (M.A. Macêdo).

http://dx.doi.org/10.1016/j.jmmm.2015.07.085
0304-8853/

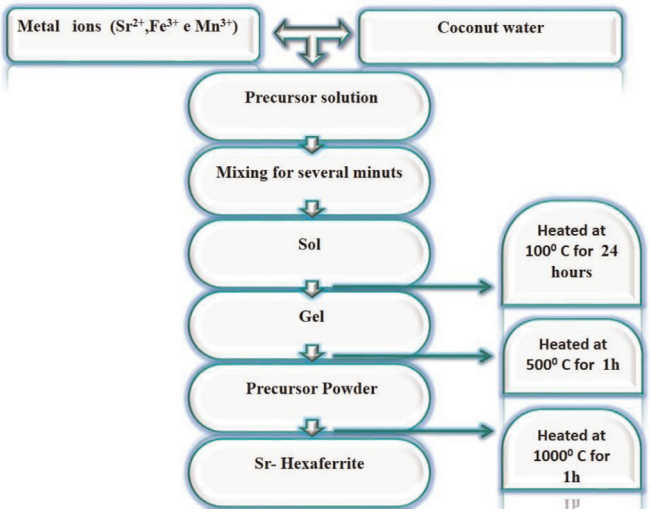

Fig. 1. Flow chart for sample preparation of Sr-hexaferrite nanopowders by the proteic sol–gel process.

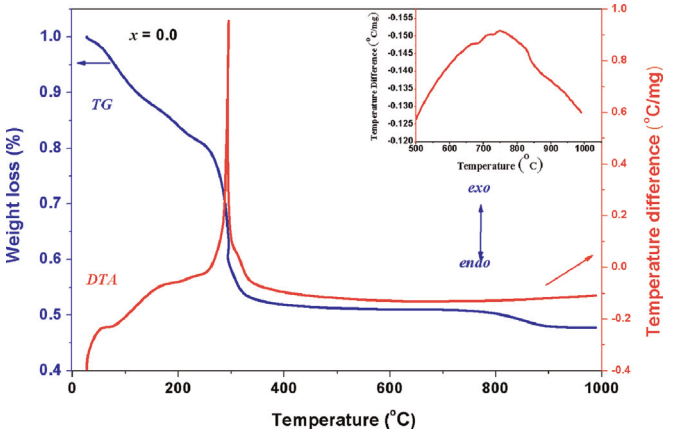

Fig. 2. Thermogravimetric (TGA) curve and differential thermal analysis (DTA) curve of the sol–gel precursor, $SrFe_{12-x}Mn_xO_{19}$ ($x=0.0$).

and $MnCl_2 \cdot 4H_2O$ (99% Sigma-Aldrich) were dissolved in filtered coconut water and mixed for several seconds to form the sol. The sol was dried at 100 °C for 24 h for gel formation and dehydration. Afterwards, it was transformed into xerogel. For the decomposition of organic materials and salts, the xerogel was calcined first at 500 °C for 1 h at a heating rate of 1 °C per minute in an open atmosphere. Then, the temperature was increased at a rate of 1 °C per minute up to a temperature of 1000 °C, where it remained for 1 h, and then the xerogel was removed from the oven at room temperature. The systematic procedure for the synthesis of hexaferrite is illustrated in Fig. 1.

2.2. Characterization

The thermal behavior of the samples was studied by thermogravimetric and differential thermal analyses (TG–DTA) using a simultaneous TG–DTA (TA Instruments) at a heating rate of 10 °C per minute in air synthetic with a flux of 100 ml/min. Fourier transform infrared (FT-IR) spectroscopy measurements of the samples were performed on a Virian Resolutions Pro in the range of 400–4000 cm^{-1} with KBr pellets. X-ray diffraction (XRD) analysis of the calcined $SrFe_{12-x}Mn_xO_{19}$ (with $x=0.0$ to 0.10) samples was performed in a Rigaku X-ray diffractometer using a Cu K_α radiation tube operated at 40 kV and 40 mA. XRD data were taken in step scan mode in the range of 20–80° (2θ) with step sizes of 0.02° and a scan speed of 0.02°/min. The structural and microstructural parameters were extracted using Rietveld refinement with the program FullProf [7]. The Bragg peaks were modeled with the pseudo-Voigt function, and the background was estimated by linear interpolation between selected background points. The determination of the average crystallite sizes (D) and the lattice microstrain (ε) was estimated by line-broadening analysis using Williamson–Hall (W–H) [8] methods. The morphology, microstructure, and particle size of the $SrFe_{12}O_{19}$ and $SrFe_{11.9}Mn_{0.10}O_{19}$ nanopowders were examined by scanning electron microscopy (SEM) using a MIRAN 3 TESCAN with an accelerating voltage of 13.0 kV. The SEM images were analyzed with the software ImageJ [9]. The magnetic properties of SrM samples were measured at room temperature using a maximum external field of 70 kOe and a Magnetic Properties Measurements System (MPMS; Quantum Design). ^{57}Fe Mössbauer effect measurements were taken at room temperature in a transmission geometry using a conventional constant-acceleration spectrometer operating in triangular wave mode with a ^{57}Co source in a rhodium matrix. The spectrometer was calibrated with a 25-μm-thick α-Fe foil.

3. Results and discussion

3.1. Thermal analysis

Fig. 2 shows the TG–DTA curve of the synthesized $SrFe_{12-x}Mn_xO_{19}$ ($x=0.0$). Thermal analysis of the sample was carried out up to 1000 °C at a heating rate of 10 °C/min in an argon gas with platinum crucibles to observe the structural variations, such as the weight loss and transformation of different phases during heat treatment. The TGA curve shows that the first mass loss occurred between 45 °C and 100 °C along with an exothermic peak at 53 °C and a slightly weak endothermic trough at 76 °C in the DTA curve, which are respectively associated with the decomposition of nitrates and the evaporation of both water molecules still present in the sample and water adsorbed from the atmosphere after the preparation of the xerogel before measurement. The second mass elimination between 150 and 258 °C is associated with the melting of proteins [10]. At temperatures of 272 and 334 °C, it was possible to observe a third mass loss associated with an exothermic peak at 293 °C due to the probable formation of hydroxides. The fourth mass loss between at 370 and 783 °C is correlated with the decomposition of hydroxides and organic matter from the precursor agents in coconut water as well as the formation of several metal oxides and mono-ferrite. The fifth exothermic peak at 754 °C suggests the formation of the hexaferrite phase (inset in Fig. 2) [11].

3.2. FT-IR spectroscopy

The spectra were recorded by mixing 0.05% in KBr powder to obtain better resolution of the bands. Fig. 3 shows the absorption bands at 435, 535, and 595 cm^{-1}, which are characteristic of hexaferrite [12,13]. The peaks at 1200, 1470, and 1560 cm^{-1} are related to the M–O–M (metal–oxygen–metal) bands, such as Fe–O–Mn and Fe–O–Fe. The presence of these bands suggests that Fe–O and Sr–O bonds could interact with Mn dopant atoms. The variation in the band positions resulted from differences in the distances between tetrahedral and octahedral sites at which they occurred in the intervals of 400–500 cm^{-1} and 500–700 cm^{-1}. This directly resulted in a shift of the absorption peaks due to variations in the distances of Fe^{3+}–O^{2-} caused by the replacement of Mn^{3+} [14]. The relatively broad peaks at 3440 cm^{-1} for both samples became narrow and are associated with the deformation vibration of hydroxyl groups (OH) obtained in a wet atmosphere.